ORIGINAL ARTICLE

# Combination treatment of cordycepin and radiation induces apoptosis accompanied by protective autophagy in TM3 mouse Leydig progenitor cells

Yu-Yan Lan [a,1], Yi-Ping Lee [b,1], Wei-Ru Huang [c,1], Chun-Ying Yu [d], Lyh-Jyh Hao [e,f], Chun-Hung Lin [g,*], Bu-Miin Huang [c,d,h,**]

[a] School of Medicine, College of Medicine, I-Shou University, Kaohsiung, Taiwan
[b] Department of Physical Therapy, Shu-Zen Junior College of Medicine and Management, Kaohsiung, Taiwan
[c] Department of Cell Biology and Anatomy, College of Medicine, National Cheng Kung University, Tainan, Taiwan
[d] Department of Biomedical Sciences, National Chung Cheng University, Chiayi, Taiwan
[e] Department of Endocrinology and Metabolism, Kaohsiung Veteran General Hospital, Tainan Branch, Tainan, Taiwan
[f] Department of Optometry, Chung Hwa University of Medical Technology, Tainan, Taiwan
[g] Department of General Surgery, Dalin Tzu Chi Hospital, Buddhist Tzu Chi Medical Foundation, Chiayi, Taiwan
[h] Department of Medical Research, China Medical University Hospital, China Medical University, Taichung, Taiwan

**Abstract**

**Leydig cells are anatomically located in the testicular interstitial tissue, and their main function is to produce and secrete testosterone and indirectly support spermatogenesis. We previously reported that the combination treatment of cordycepin and radiation can effectively induce Leydig tumor cell apoptosis through cell cycle arrest, caspase activation, endoplasmic reticulum (ER) stress, reactive oxygen species (ROS) accumulation, and DNA damage. However, there is still a lack of scientific evidence for the susceptibility of normal Leydig cells to the combination treatment. In the present study, mouse TM3 Leydig progenitor cells were used as a model to evaluate the effects and mechanisms of the combination treatment on normal Leydig cells. It was found that 2-fold higher concentration of cordycepin (50 μM) plus 1.5-fold higher dosage of radiation (6 Gy) induce death-related morphological changes and reduce cell viability to a similar extent in TM3 cells as compared to the effects on MA-10 Leydig tumor cells. The treated TM3 cells showed a significant augmented percentage in sub-G1 and G2/M phases with a decreased percentage of G1 and S phase in the cell cycle progression. Interestingly, protective autophagy with the regulation of autophagy-related proteins, including an increase in LC3 conversion, Atg5 and Atg12-Atg5 expressions, and a decrease in Beclin-1 expression were observed in TM3 cells following the combination treatment. However, p62 accumulation became more pronounced over time after 24 h of treatment, accompanied by a rising percentage of apoptotic cells. In conclusion, normal Leydig cells show higher resistance to the combination treatment of cordycepin and radiation than Leydig tumor cells. Although apoptosis is eventually induced in TM3 cells, protective autophagy is also activated to mitigate the cytotoxic impact of the combination treatment. This finding may provide a reference for the development of safe therapeutic regimen for Leydig cell tumors.**

*Keywords:* Apoptosis, Autophagy, Cordycepin, Radiotherapy, TM3 cell Leydig progenitor cells

## 1. Introduction

Leydig cells are located in the interstitial tissue of the male testes, and their main biological function is to produce and secrete testosterone which is an essential steroid for spermatogenesis, development of male reproductive organs, and maintenance fertility through binding to androgen

Received 19 August 2025; accepted 1 October 2025.
Available online 15 December 2025

* Corresponding author at: Department of General Surgery, Dalin Tzu Chi Hospital, Buddhist Tzu Chi Medical Foundation, #2, Ming-Shan Road, Dalin, Chiayi, Taiwan.
** Corresponding author at: Department of Biomedical Sciences, National Chung Cheng University, No. 168, Section 1, University Road, Ming-Hsiung, Chiayi, 621301, Taiwan.
E-mail addresses: linch51.leo@gmail.com (C.-H. Lin), bmhuang66@gmail.com (B.-M. Huang).
[1] Contributed equally.

https://doi.org/10.38212/2224-6614.3567

receptors [1–3]. These cells and their secreted factors, such as testosterone and insulin-like growth factor 1 (IGF1), also play a crucial role in Sertoli cell development, peritubular cell differentiation, and seminiferous tubule contractions to promote sperm transfer and ensure fertility [4,5]. Therefore, dysfunction or malignancy of Leydig cells will seriously reduce male reproductive ability.

Leydig cell tumor, the most prevalent non-germ cell tumor in the testis, is classified as a sex cord-stromal tumor [6,7]. In clinical practice, radical orchiectomy is commonly used to treat Leydig cell tumors [8]. Unfortunately, this procedure can result in permanent damage to male reproductive ability [9]. Radiotherapy is a conventional cancer treatment which can induce cancer cell apoptosis through direct and indirect mechanisms, including the induction of DNA breakage and the accumulation of reactive oxygen species (ROS), respectively [10–12]. Since the testes are highly sensitive to radiation, doses above 4 Gy can lead to azoospermia in most men [13]. Therefore, combining it with ideal chemotherapeutic agents capable of a synergistic effect is necessary to enhance its clinical applicability. Cordycepin, a predominant bioactive component of *Cordyceps sinensis*, has been reported to have pharmacological effects against various cancers including melanoma, lung cancer, oral cancer, breast cancer, prostate cancer, and testicular cancer, based on its superior ability to modulate different biological mechanisms, such as immunity, cell cycle, oxidative stress, autophagy, and apoptosis [14–16]. We have previously demonstrated that cordycepin enhances radiosensitivity by modulating the cell cycle, caspase pathway, and endoplasmic reticulum (ER) stress, ultimately leading to apoptosis in MA-10 mouse Leydig tumor cells [17]. Furthermore, the combination treatment of cordycepin and radiation also induced ROS accumulation to cause DNA damage on MA-10 cells [18]. In these studies, combining 25 μM cordycepin with 4 Gy radiation killed approximately half of the MA-10 cells *in vitro* [17,18]. However, there is insufficient scientific evidence on the impact of combining cordycepin and radiation on normal Leydig cells. Therefore, it is important to identify the optimal cordycepin concentration and radiation dosage that induce Leydig tumor cell death with minimal impact on normal Leydig cells. Additionally, understanding how the combination treatment affects Leydig tumor cells differently from normal Leydig cells is crucial for future clinical applications.

The cell cycle is a sequence of events in a cell that ultimately drives the cell to divide into two daughter cells [19]. The typical cell cycle consists of G1, S, G2, and M phases, which are critical for cell proliferation, growth, and repair [20]. The cell cycle-related proteins, cyclin-dependent kinases (Cdks) and cyclins, dominate the regulation of cell cycle progression [21]. Any therapeutic strategy that causes DNA damage may alter cell cycle progression, and the modulated consequences will affect the sensitivity of cells to therapeutic strategies [19,22]. Therefore, the impact on the cell cycle should be considered when evaluating the efficacy and safety of therapeutic strategies. In the cell cycle, the presence of the Sub-G1 phase indicates cells with DNA content lower than that of the G1 phase, typically due to DNA damage or apoptosis [23]. When cells enter the G2/M phase, the cells will check whether the DNA integrity is sufficient for mitosis, if not, the repair mechanism will be initiated. When the DNA damage is too severe to be repaired, G2/M arrest will occur, and the apoptosis mechanism will be initiate to avoid passing the damage to the daughter cells [24]. This situation may also lead to a reduction in the ratio of cells in the G1 and S phases [19]. In our previous study, prolonged sub-G1 and G2/M arrest accompanied by the regulation of cell cycle-related proteins were observed in MA-10 mouse Leydig tumor cells following the combination treatment of 25 μM cordycepin and 4 Gy radiation [17]. However, whether the combination treatment affects the cell cycle of normal Leydig cells remains unknown.

Autophagy is a stress-induced catabolic process that can transport damaged organelles or misfolded proteins to lysosomes for degradation [25]. It can also respond to various cytotoxic injuries and promote cell survival [26]. However, dysregulation of autophagosome content degradation may sometimes result in cell death [26,27]. Generally, autophagy initiates with the formation of the Unc-51-like kinase 1 (Ulk1)-RB1-inducible coiled-coil protein 1 (FIP200)- autophagy-related protein (Atg)13 complex induced by cellular stress. It is further assisted by vacuolar protein sorting 34 (VPS34), Beclin-1, Atg9 and other molecules to first form a meniscus bilayer membrane structure, called phagophore. With the assistance of two ubiquitin-conjugation systems, Atg12-Atg5-Atg16 complex and phosphatidylethanolamine (PE)-conjugated microtubule-associated protein light chain 3 (LC3) II system, the phagophore gradually elongates and transforms into an autophagosome with accumulated cytosolic contents. Subsequently, the autophagosome fuses with the lysosome, and the acid hydrolase in the lysosome degrades the autophagic cargo. Useful nutrients can be recycled and

released back to the cytoplasm for reuse by the cell [28]. Notably, p62, a multifunctional adapter protein that has the function of connecting the autophagosome and the ubiquitin degradation system, can bind to ubiquitinated proteins and connect them to LC3 II to promote their degradation during autophagic process [29]. However, recent reports indicate that accumulation of p62 leads to apoptosis [30], possibly through deactivation of mechanistic target of rapamycin complex 1 (mTORC1) or induction of oxidative stress [31]. Furthermore, the complex formed by p62 and LC3 II can activate the pro-apoptotic factor BH3-interacting domain death agonist (BID) [29]. Activated BID may further initiate mitochondria-mediated apoptosis by triggering the release of cytochrome *c* [29,32]. It is important to gain a deeper understanding of the ability of the combination treatment of cordycepin and radiation to induce autophagy in Leydig cells and whether the consequences are directed toward cell survival or apoptosis.

Apoptosis is pivotal in determining the fate of cells [33]. Following the initiation of autophagy, cells may either inhibit or promote apoptosis, or they may proceed independently of each other [27]. Apoptosis can be divided into two major forms including intrinsic and extrinsic pathways based on the triggering mechanism [34,35]. Intrinsic apoptosis pathway is initiated by various stress conditions, including DNA damage, hypoxia, growth factor deprivation, or ER stress, and the process is regulated by anti-apoptotic and pro-apoptotic Bcl-2 family proteins. Stress-induced signal transduction can activate downstream mediators and lead to the release of apoptotic factors such as cytochrome *c*, endonuclease G, and apoptosis-inducing factor (AIF). Cytochrome *c* and caspase 9 precursors combine with apoptotic protease activating factor-1 (APAF-1) to form the apoptosome, subsequently triggering the cleavage and activation of caspase 9. Extrinsic apoptosis pathway is initiated through the binding of death receptors and corresponding ligands, such as Fas and Fas ligand (FasL). This engagement leads to the formation of a receptor-associated complex consisting of Fas-associated death domain (FADD) and caspase 8 and 10, resulting in the cleavage and activation of caspase 8 and 10. Both intrinsic and extrinsic apoptotic pathways ultimately induce the cleavage and activation of caspase 3, which further cleaves and activates polyADP-ribose polymerase (PARP), leading to cell death [34,35]. Once apoptosis occurs, the DNA in the cell nucleus is fragmented, and changes concurrently occur in the cell membrane which characterized by phosphatidylserine flipping [36,37]. Our previous report has shown that the combination treatment of cordycepin and radiation can effectively induce apoptosis in Leydig tumor cells [17], but the impact on normal Leydig cells urgently needs evidence support.

TM3 cell, a murine Leydig progenitor cell derived from an immature BALB/c mouse, has been isolated and extensively propagated in cell culture for numerous years [38]. Notably, since tumor formation does not occur when TM3 cells are injected into BALB/c *nu/nu* mice, this model can be regarded as a normal cell model [39]. This cell line has been used in many previous studies to address the cellular toxicity exerted by different chemicals, growth factors or drugs such as butylated hydroxytoluene [40], fibroblast growth factor 9 [41], and Tripterygium glycoside tablets [42]. Therefore, present study aimed to investigate the toxicological events and mechanisms occurring in TM3 Leydig progenitor cells treated with cordycepin, radiation and their combination.

Our findings reveal that Leydig progenitor cells are more resistant than Leydig tumor cells to the combination treatment of cordycepin and radiation. Although the treatment still induces Leydig progenitor cells to eventually undergo apoptosis through cell cycle arrest and p62 accumulation under relatively higher dosage condition, protective autophagy is initiated in the early stages post treatment to reduce the cytotoxic impact on normal Leydig cells. These results provide a scientific basis for the application of combining cordycepin and radiation in Leydig tumor treatment.

## 2. Materials and methods

### 2.1. Cell culture

TM3 mouse Leydig progenitor cell line (cat. no. CRL-1714) was purchased from ATCC (Manassas, VA, USA). Cells were cultured in Dulbecco's modified Eagle's medium (DMEM)/F12 (cat no. 12400-024, Thermo Scientific, Waltham, MA, USA) supplemented with 5% horse serum (cat no. 26050070, Thermo Scientific, Waltham, MA, USA), 2.5% fetal bovine serum (cat no. 10437-028, Thermo Scientific, Waltham, MA, USA), 100 IU/ml penicillin and 100 μg/ml streptomycin (cat no. CC502-0100, Simply Biologics, Redmond, WA, USA) in a humidified incubator containing 5% $CO_2$ at 37 °C.

### 2.2. Chemicals

Cordycepin and dimethyl sulfoxide (DMSO) (cat. no. D4540-500 ML, Sigma–Aldrich, St. Louis, MO,

USA) were purchased from Sigma–Aldrich. The purities of the cordycepin identified by high-performance liquid chromatography is more than 98%. The cordycepin was dissolved in DMSO to 80 mM for stock. The stock solution is further diluted with cell culture medium to working concentrations for all experiments.

### 2.3. Radiation treatment

Radiation treatment was administered using a linear accelerator (Siemens Medical Systems, Malvern, PA, USA) with a 6 MV X-ray source. TM3 cells cultured in 25T tissue culture flasks were irradiated at a dose rate of 5 Gy/min for varying durations. To ensure electronic equilibrium, an additional 2 cm of tissue-equivalent bolus was placed on top of the flask, while 10 cm of tissue-equivalent material was placed beneath the tissue culture flask to achieve full backscatter.

### 2.4. Cell morphology observation

TM3 cells were seeded at a density of $3 \times 10^5$ cells/ml in 25T flasks containing 4 ml of culture medium. After attachment, cells were then treated with varying concentrations of cordycepin (10, 25, 50, and 100 μM) and radiation doses (2, 4, 6, and 8 Gy) either individually or in combination for 24 h. Cell morphology was examined using an Olympus CK40 light microscope (Olympus Corporation, Tokyo, Japan), and images were captured with an Olympus DP20 digital camera (Olympus Corporation).

### 2.5. Trypan blue exclusion assay

TM3 cells were seeded at a density of $3 \times 10^5$ cells/ml in 25T flasks with 4 ml of culture medium. After attachment, cells were then treated with varying concentrations of cordycepin (10, 25, 50, and 100 μM) and radiation doses (2, 4, 6, and 8 Gy) either individually or in combination for 24 h. In addition, for the autophagy inhibition experiment, TM3 cells were preincubated without or with 10 or 50 μM autophagy inhibitor, chloroquine (CQ), for 1 h and then treated without or with 50 μM cordycepin, 6 Gy radiation, or 50 μM cordycepin plus 6 Gy radiation for additional 24 h. The cells were detached using trypsin and mixed with an equal volume of 0.4% trypan blue solution. Stained (dead) and unstained (live) cells were counted using a hemocytometer, and cell viability was calculated as the percentage of live cells.

### 2.6. Treatment interaction assessment

The synergistic, additive, or antagonistic effects of the combination treatment of cordycepin and radiation on TM3 cells were evaluated using the combination index (CI) method with CalcuSyn software version 2.0, based on the median effect model [43]. Experimental data were input into the CalcuSyn interface to compute CI values. A CI value less than 1 indicates synergistic interaction, equal to 1 suggests additive effects, and more than 1 signifies antagonistic interaction between the two treatments.

### 2.7. Cell cycle analysis

The cell cycle distribution was assessed using propidium iodide (PI) staining followed by flow cytometric analysis. TM3 cells were treated with or without 50 μM cordycepin, 6 Gy radiation, or their combination for 3, 6, 9, 12, and 24 h. After treatment, cells were detached with trypsin, fixed in 70% ethanol at 4 °C for 24 h, and then incubated with 100 μg/ml ribonuclease. Subsequently, samples were stained with 40 μg/ml PI for 30 min and analyzed using CytoFLEX flow cytometry (Beckman Coulter, Brea, CA, USA) with CytExpert software version 2.0 (Beckman Coulter) under an excitation wavelength of 488 nm and bandpass filters of 600 nm conditions.

### 2.8. Autophagy detection

TM3 cells were treated with or without 50 μM cordycepin, 6 Gy radiation, or their combination for 12, and 24 h. After treatment, cells were harvested and strained with 1 μg/ml acridine orange in the dark for 20 min to detect acidic vesicular organelles (AVOs). Green (510–530 nm) and red (>650 nm) fluorescence emission from cells illuminated with blue (488 nm) excitation light was measured using CytoFLEX flow cytometry (Beckman Coulter) with CytExpert software version 2.0 (Beckman Coulter). When autophagy activity increases, the number and/or size of AVOs increases, resulting in an increase in red fluorescence. Red fluorescent positive cells are counted as autophagic cells.

### 2.9. Protein extraction and western blotting

TM3 cells were seeded at a density of $3 \times 10^5$ cells/ml in 25T flasks containing 4 ml of culture medium. After attachment, cells were then treated with varying concentrations of cordycepin

(10, 25, 50, and 100 μM) and radiation (2, 4, 6, and 8 Gy) doses either individually or in combination for 3, 6, 9, 12, or 24 h, respectively. Cells were harvested, washed with cold phosphate buffered saline, pelleted by centrifuging at 700×*g* for 5 min, and then lysed using 100 μl of RIPA lysis buffer (cat no. 89900, Thermo Scientific, Waltham, MA, USA) with Halt protease inhibitor cocktail (cat no. 87786, Thermo Scientific, Waltham, MA, USA) and incubated at room temperature for 30 min. After lysis, cell debris was removed by centrifugation at 12,000×*g* for 12 min at 4 °C. The supernatants were collected and stored at −20 °C for subsequent analysis. Protein concentrations in the cell lysates were determined using the Bio-Rad protein assay dye reagent concentrate (cat no. 5000006, Bio-Rad, Hercules, CA, USA) following the manufacturer's instructions. For western blotting analysis, protein samples (25 μg/lane) were loaded onto a 12% sodium dodecyl sulfate-polyacrylamide gel in standard running buffer at room temperature. Subsequently, proteins were electrophoretically transferred onto a polyvinyldifluoride (PVDF) membrane at 4 °C. The PVDF membrane (cat. no. BSP0161, PALL Corporation, Port Washington, NY, USA) was blocked with 5% nonfat milk and then washed with tris-buffered saline containing 0.1% Tween 20 (cat. no. 123412-1611, PanReac AppliChem, Iselin, NJ, USA). The membrane was then incubated overnight at 4 °C with primary antibodies against LC3 A/B (cat. no. 12741, monoclonal rabbit IgG, 1:1000 dilution, Cell Signaling, Boston, MA, USA), β-actin (cat. no. A5441, monoclonal mouse IgG, 1:8000 dilution, Sigma−Aldrich, St. Louis, MO, USA), Atg5 (cat. no. 12994, monoclonal rabbit IgG, 1:2000 dilution, Cell Signaling, Boston, MA, USA), Atg12 (cat. no. 4180, monoclonal rabbit IgG, 1:2000 dilution, Cell Signaling, Boston, MA, USA), or Beclin-1 (cat. no. 3495, monoclonal rabbit IgG, 1:1000 dilution, Cell Signaling, Boston, MA, USA). After washing, the membrane was incubated with horseradish peroxidase (HRP)-conjugated secondary antibodies: goat anti-mouse IgG (cat. no. NEF82200-1 EA, 1:2000 dilution, PerkinElmer, Waltham, MA, USA) or goat anti-rabbit IgG (cat. no. NEF81200-1 EA, 1:2000 dilution, PerkinElmer) for 1 h at room temperature. Protein bands were visualized using an enhanced chemiluminescence kit (cat. no. WBKLS0500, Merck Millipore, Burlington, MA, USA) and the UVP EC3 BioImaging System (Phoenix, AZ, USA). The intensity of each protein band was quantified using ImageJ software version 1.50, with β-actin levels as a control for normalizing protein expression.

### *2.10. Apoptosis detection*

TM3 cells were treated with or without 50 μM cordycepin, 6 Gy radiation, or their combination for 24, 48 and 72 h, respectively. Cellular apoptosis was assessed using the fluorescein isothiocyanate (FITC) Annexin V apoptosis detection kit (BD Pharmingen, San Diego, CA, USA), following the manufacturer's instructions. Samples were evaluated using a CytoFLEX flow cytometer (Beckman Coulter) equipped with CytExpert software (Beckman Coulter). Fluorescence was excited at 488 nm, and emission was captured through bandpass filters set at 515 nm for FITC and 600 nm for PI detection. The data were visualized as histogram plots and categorized into four quadrants based on staining patterns including double-negative (Annexin V-/PI-), PI single-positive (Annexin V-/PI+), Annexin V single-positive (Annexin V+/PI-), and double-positive (Annexin V+/PI+), which corresponded to viable, necrotic, early apoptotic, and late apoptotic cells, respectively.

### *2.11. Statistical analysis*

The data are expressed as mean ± standard error of the mean (SEM) of three independent experiments. Statistically significant differences were determined by one-way or two-way analysis of variance (ANOVA) with Dunnett's or Tukey's test for multiple comparisons. The statistical significance was considered as $P < 0.05$ in all experiments.

## 3. Results

### *3.1. Cordycepin and radiation induce morphological changes and reduce cell growth density in TM3 cell cultures*

To evaluate the toxicity of cordycepin, radiation, and their combination treatment on TM3 Leydig progenitor cells, we conducted three series of experiments that treating TM3 cells with either cordycepin (10−200 μM), radiation (2−8 Gy), or their combination under different arrangements. After 24 h of treatment, cell morphological change was examined under a light microscope and images were captured with a digital camera. In the experiment with cordycepin alone treatment (Fig. 1A−F), untreated control TM3 cells adhered firmly to the bottom plane of culture flask and displayed the expected spindle-shaped morphology. Conversely, TM3 cells treated with increasing doses of cordycepin gradually became rounder and more

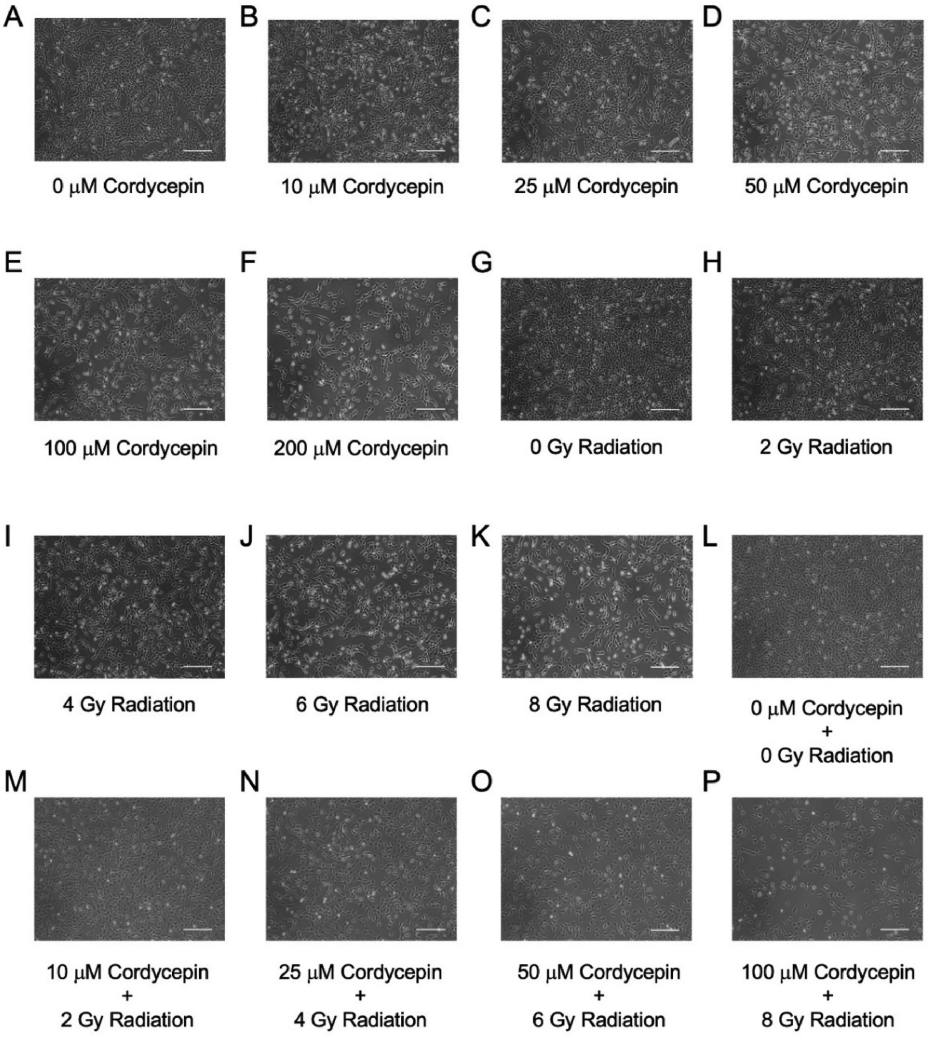


*Fig. 1. Cordycepin and radiation induce morphological changes and reduce cell growth density in TM3 cell cultures. TM3 cells were treated (A−F) with 0, 10, 25, 50, 100, or 200 μM cordycepin for 24 h; (G−K) with 0, 2, 4, 6, or 8 Gy radiation for 24 h; or (L−P) with the combination of cordycepin and radiation under 0 μM cordycepin plus 0 Gy radiation, 10 μM cordycepin plus 2 Gy radiation, 25 μM cordycepin plus 4 Gy radiation, 50 μM cordycepin plus 6 Gy radiation, or 100 μM cordycepin plus 8 Gy radiation conditions for 24 h, respectively. Cell morphology and growth density were observed using phase contrast microscopy and images were captured by digital camera (scale bar, 100 μm). The experiment was repeated three times, and a representative result is presented.*

separated. In the experiment with radiation treatment alone (Fig. 1G−K), the morphological changes in TM3 cells were similar to those in cordycepin-treated cells. The number of rounded cells increased, and adherent cells decreased progressively from receiving 2−8 Gy radiation treatments. These results indicate that both cordycepin and radiation treatments induce morphological changes associated with cell death and reduce cell growth density in TM3 cell cultures. Furthermore, in the experiment with combination treatment under different conditions (Fig. 1L−P), the relatively high-dose combinations (50 μM cordycepin plus 6 Gy radiation and 100 μM cordycepin plus 8 Gy radiation) showed a more obvious decrease in viable cell density than the corresponding single treatment groups, suggesting that combining the two treatments under these conditions may have an additive or synergistic effect on TM3 cells.

### *3.2. Cordycepin and radiation decrease cell viability of TM3 cells in a dose-dependent manner*

To further quantify the cell death-inducing capabilities of cordycepin, radiation, and their combination treatment on TM3 cells, we utilized the Trypan blue exclusion assay to analyze cell viability and following the CI values were calculated by using CalcuSyn software to assess the interaction of the treatments. The results showed that the cell

viability percentages of TM3 cells treated with cordycepin at concentrations of 10–200 μM (Fig. 2A) or radiation at doses of 4–8 Gy (Fig. 2B) for 24 h, as baseline dose, were significantly reduced in a dose-dependent manner ($P < 0.05$). In addition, combination treatment with cordycepin and radiation at conditions of 25 μM plus 4 Gy, 50 μM plus 6 Gy, and 100 μM plus 8 Gy for 24 h led to significant reductions in TM3 cell viability to 70%, 50%, and 38%, respectively ($P < 0.05$) (Fig. 2C). The CI values calculated by CalcuSyn software of the combination treatments at 50 μM plus 6 Gy and 100 μM plus 8 Gy are 0.976 (c point) and 0.991 (d point), respectively, indicating an additive or synergistic effect on reducing TM3 cell viability under these two conditions (Fig. 2D). Based on the combination dose at 50 μM cordycepin plus 6 Gy radiation is close to the half-maximal inhibitory concentration ($IC_{50}$) value on TM3 cell viability inhibition, this condition was selected for further mechanistic investigation in the present study. Importantly, compared to previous research finding, it requires 1.5-fold higher radiation dosage and 2-fold higher cordycepin concentration to induce cell death in TM3 Leydig progenitor cells compared to MA-10 Leydig tumor cells as combination treatment of 25 μM cordycepin plus 4 Gy radiation is the $IC_{50}$ value on MA-10 cell viability inhibition (control group) [17], supporting that Leydig progenitor cells are more resistant to the inhibitory effects on cell viability caused by the combination treatment than Leydig tumor cells.

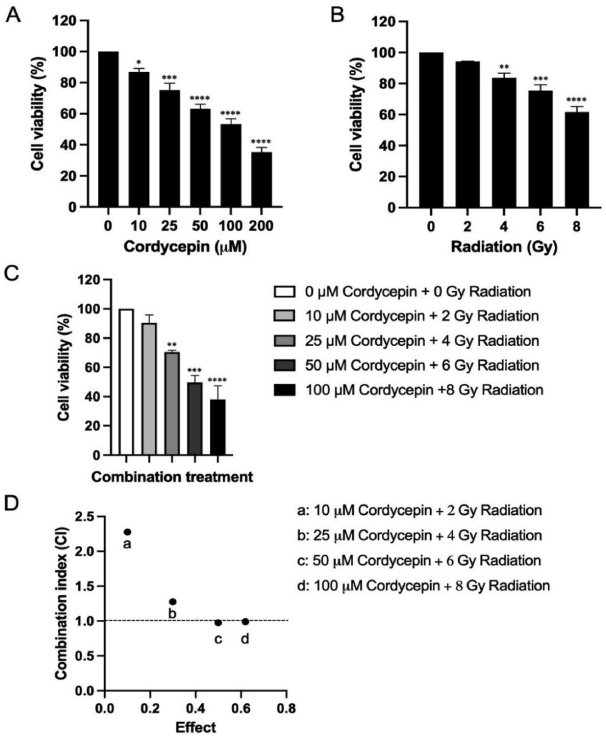


*Fig. 2. Cordycepin and radiation decrease cell viability of TM3 cells in a dose-dependent manner. TM3 cells were treated (A) with 0, 10, 25, 50, 100, and 200 μM cordycepin for 24 h, (B) with 0, 2, 4, 6, and 8 Gy radiation for 24 h, or (C) with the combination of cordycepin and radiation under 0 μM cordycepin plus 0 Gy radiation, 10 μM cordycepin plus 2 Gy radiation, 25 μM cordycepin plus 4 Gy radiation, 50 μM cordycepin plus 6 Gy radiation, and 100 μM cordycepin plus 8 Gy radiation conditions for 24 h, respectively. Cell viabilities were determined by Trypan blue exclusion assay. Data are presented as mean ± SEM of three independent experiments in percentages of cell viability relative to the control group. *$P < 0.05$, **$P < 0.01$, ***$P < 0.001$, and ****$P < 0.0001$ indicate significant statistical difference compared to the control group. (D) Combination index (CI) was calculated by using CalcuSyn software. The dashed line represents the CI equal to 1. A CI of less than, equal to, and more than 1 indicates synergistic, additive, and antagonistic interaction of two treatments, respectively.*

### 3.3. Cordycepin and radiation regulate cell cycle distribution in TM3 cells

Regulation of the cell cycle is crucial to cell viability [23]. To determine whether cordycepin and radiation caused cell viability reduction in TM3 cells is due to cell cycle regulation, TM3 cells treated without or with cordycepin, radiation, or their combination were stained with PI and the DNA contents were analyzed by flow cytometry. Fig. 3A demonstrates the distinct patterns in DNA content between the treated groups and the control group, particularly, the changes on the cell cycle patterns are most pronounced in the groups that TM3 cells receiving radiation and combination treatment. The quantitative results indicate that treatment with cordycepin, radiation, or their combination potentially increases the proportion of TM3 cells in the sub-G1 and G2/M phases, while reducing the proportion in the G1 and S phases (Fig. 3B–E). In detail, the proportion of cells in the sub-G1 phase was significantly increased in the combination treatment group at 12 h ($P < 0.05$), suggesting the occurrence of DNA fragmentation in TM3 cells after receiving the combination treatment (Fig. 3F). The proportion of cells in the G1 phase significantly decreased at 3 and 6 h in both the radiation and combination treatment groups ($P < 0.05$) (Fig. 3G). A significant decrease in the proportion of cells in the S phase at 12 h was observed in the combination treatment group, as well as in the individual treatment groups ($P < 0.05$) (Fig. 3H). Moreover, G2/M phase arrest occurred at 6 and 9 h in the radiation and combination treatment group, respectively ($P < 0.05$), suggesting that these cells may undergo apoptosis subsequently (Fig. 3I).

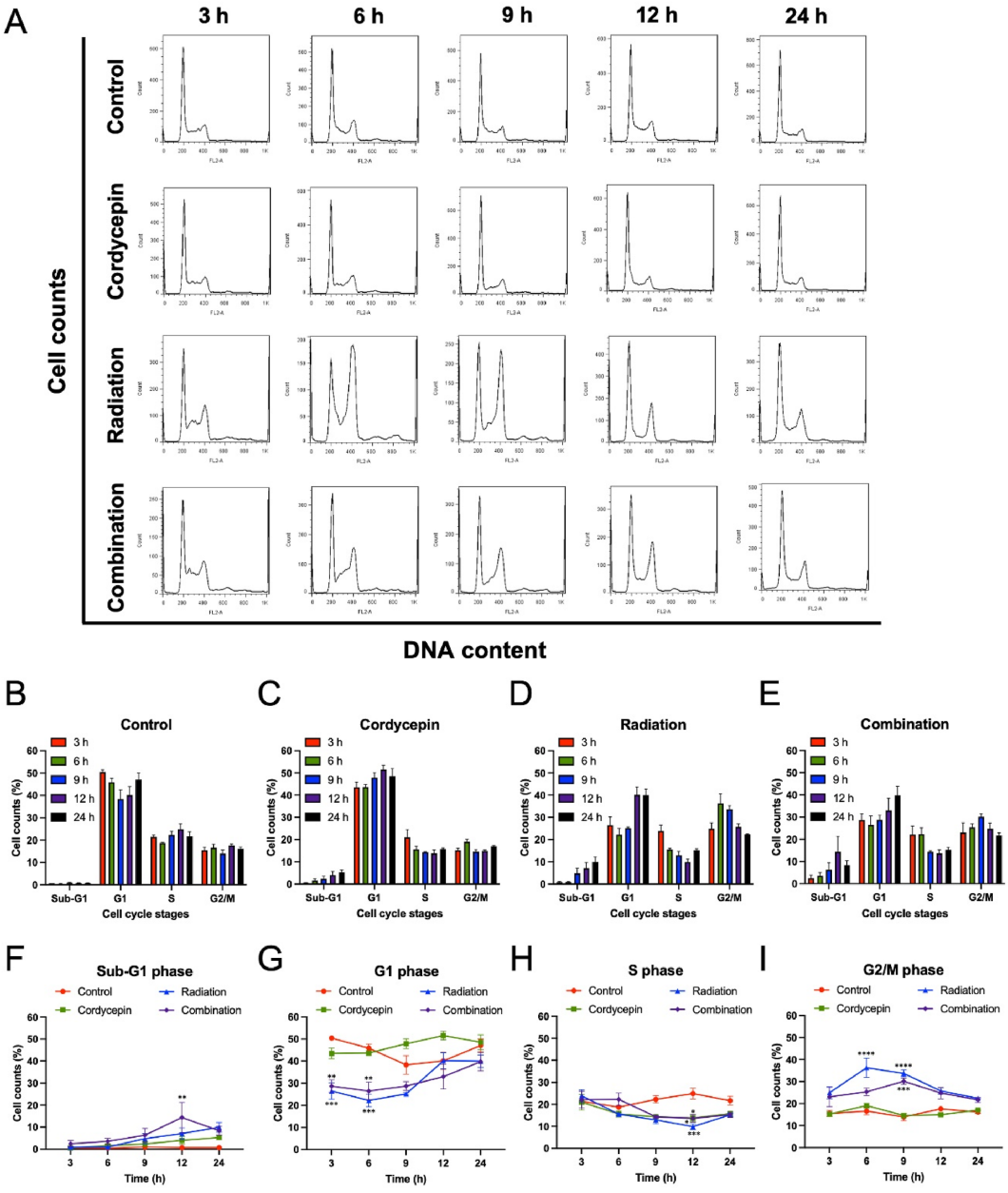


*Fig. 3. Cordycepin and radiation regulate cell cycle distribution in TM3 cells. TM3 cells were treated without or with 50 μM cordycepin, 6 Gy radiation, or 50 μM cordycepin plus 6 Gy radiation for 3, 6, 9, 12, and 24 h, respectively. Cells were fixed and stained with propidium iodide, and cell cycle was measured using flow cytometry. The experiment was repeated three times, and (A) a representative result is presented. The horizontal axis represents DNA content, and the vertical axis shows the cell counts. (B–E) The distribution of cells in sub-G1, G1, S and G2/M phase of the TM3 cells treated without or with 50 μM cordycepin, 6 Gy radiation, or 50 μM cordycepin plus 6 Gy radiation at different time points are illustrated. (F–I) The curves depicting the changes in the percentage of cells over time in the Sub-G1, G1, S, and G2/M phases for different treatment groups are shown. Data are presented as mean ± SEM of three independent experiments. *P < 0.05, **P < 0.01, ***P < 0.001, and ****P < 0.0001 indicate significant statistical difference compared to the control group.*

### *3.4. Cordycepin and radiation induce autophagy in TM3 cells*

Autophagy is a cellular process involving the degradation and recycling of proteins and organelles to maintain cellular homeostasis [27]. Both cordycepin and radiation have been reported to induce autophagy in treated cells [44,45]. When autophagy activity increases, the number and/or size of acidic vesicular organelles (AVOs) will increase. To understand whether treatment with cordycepin, radiation or their combination can

induce autophagy in TM3 cells, we used acridine orange (AO) staining to determine the extent of autophagy. Incorporating AO into AVOs results in intensified red fluorescence, indicating heightened autophagy activity. A representative experimental result shows that treatment with 6 Gy radiation plus 50 μM cordycepin induced autophagy rate of 31% at 12 h and 70% at 24 h, which were higher than those observed with cordycepin alone (18% at 12 h and 38% at 24 h), radiation alone (19% at 12 h and 30% at 24 h), and untreated control (6% at 12 h and 4% at 24 h) groups, respectively (Fig. 4A). Statistical analysis of three independent experiments reveals a significant increase in the percentage of autophagic cells among TM3 cells treated with cordycepin, radiation, or their combination, compared to the control group at 12 and 24 h, respectively ($P < 0.05$) (Fig. 4B).

### 3.5. Autophagy inhibition aggravates cordycepin and radiation-induced cell death in TM3 cells

Autophagy normally serves as a protective mechanism for cells, but disruption or excess of autophagy flux can also lead to cell death [27]. To elucidate whether autophagy induced by cordycepin, radiation, or their combination either protects TM3 cells from death or promotes cell death, we utilized CQ, a classic autophagy inhibitor that impedes the fusion of autophagosomes with lysosomes. TM3 cells were pre-incubated with CQ for 1 h to inhibit autophagy, and then cell viability under treatments with cordycepin, radiation, or their combination was assessed using the Trypan blue exclusion assay at 24 h. Consistent with the data in Fig. 2, in groups without CQ pre-incubation, treatments with cordycepin, radiation, or their combination significantly inhibited TM3 cell viability compared to the untreated control group ($P < 0.05$) (Fig. 5). Notably, the cell viability of TM3 cells treated with cordycepin, radiation, or their combination was significantly reduced when cells pre-incubated with 50 μM CQ compared to those without CQ pre-incubation ($P < 0.05$) (Fig. 5). These findings indicate that inhibition of autophagy enhances cytocidal effect induced by cordycepin, radiation, or their combination, confirming that autophagy induction is protective in TM3 cells.

### 3.6. Cordycepin and radiation regulate autophagy-related protein expressions in TM3 cells

To better elucidate the molecular involvement of the protective autophagy induced by cordycepin and radiation in TM3 cells, western blotting was

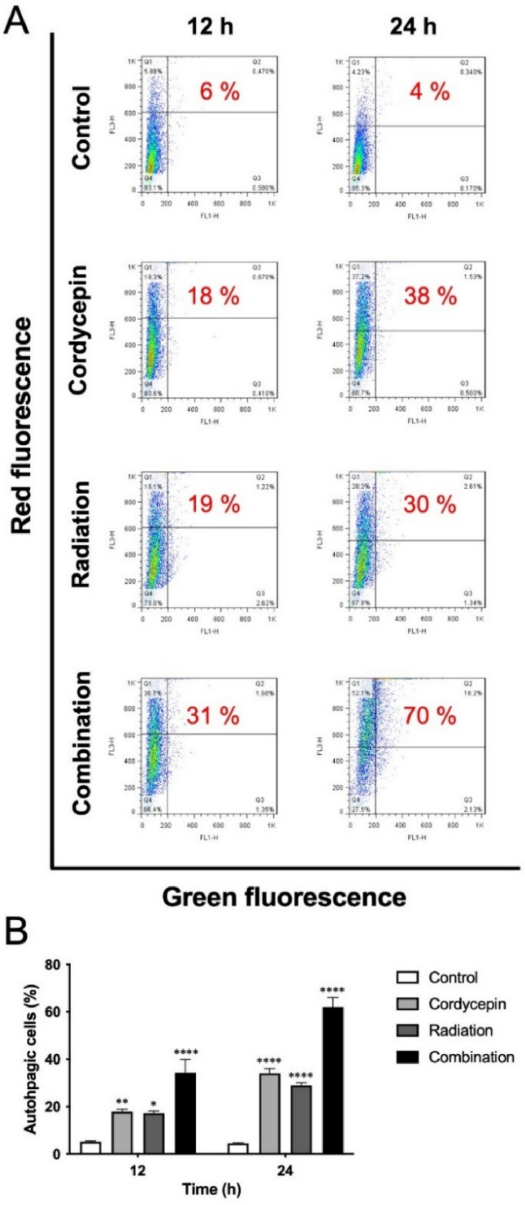


*Fig. 4. Cordycepin and radiation induce autophagy in TM3 cells. TM3 cells were treated without or with 50 μM cordycepin, 6 Gy radiation, or 50 μM cordycepin plus 6 Gy radiation for 12 and 24 h, respectively, and stained with acridine orange (AO). The green and red fluorescence intensity of AO-stained cells were measured by flow cytometry. The experiment was repeated three times, and (A) the original density plots of a representative result are presented. The horizontal axis represents the green fluorescence intensity, and the vertical axis shows the red fluorescence intensity. The red numbers represent the percentage of autophagic cells calculated from the sum of the upper left and upper right quadrants. (B) The percentages of autophagic cells in different treatment groups from three independent experiments were calculated, and data are presented as mean ± SEM. *P < 0.05, **P < 0.01, and ****P < 0.0001 indicate significant statistical difference compared to the control group.*

employed to analyze the expression levels of autophagy-related proteins LC3 I, LC3 II, Atg5, Atg12-Atg5 complex, and Beclin-1 in different time points (Fig. 6A). The results showed significant elevated

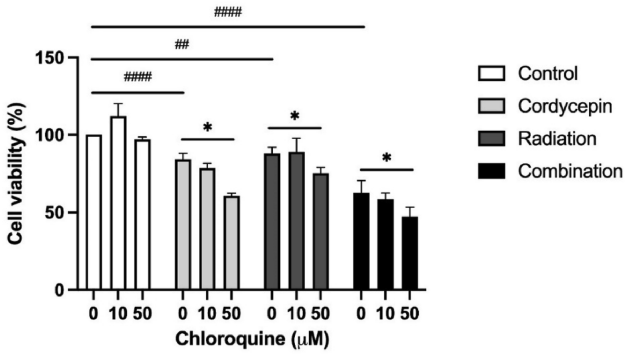


*Fig. 5. Autophagy inhibition aggravates cordycepin and radiation-induced cell death in TM3 cells. TM3 cells were preincubated without or with 10 or 50 μM chloroquine (CQ) for 1 h and then treated without or with 50 μM cordycepin, 6 Gy radiation, or 50 μM cordycepin plus 6 Gy radiation for additional 24 h. Cell viabilities were determined by Trypan blue exclusion assay. Data are presented as mean ± SEM of three independent experiments in percentages of cell viability relative to the group of control without CQ-preincubation. *P < 0.05 indicates significant statistical difference compared to the 0 μM CQ-preincubation group under individual treatment conditions. ##P < 0.01, and ####P < 0.0001 indicate significant statistical difference compared to the 0 μM CQ-preincubation, untreated control group.*

levels of the LC3 II/I ratio at 6, 9, and 24 h (Fig. 6B), Atg5 expression at 3 and 12 h (Fig. 6C), and Atg12-Atg5 complex expression at 3 h (Fig. 6D) in TM3 cells following treatment with the combination of cordycepin and radiation compared to the control group ($P < 0.05$). However, the expression of Beclin-1 was significantly decreased at 6, 9, and 24 h ($P < 0.05$) (Fig. 6E). These findings clearly demonstrate that the combination treatment-induced protective autophagy is accompanied by regulation of the expression of autophagy-related proteins in TM3 cells.

### *3.7. Cordycepin and radiation induce p62 protein accumulation in TM3 cells*

The stress-inducible autophagy-related protein p62, located in cytosolic speckles, plays a crucial role in regulating cell survival or death by recruiting and oligomerizing essential signaling molecules [30]. When p62 accumulates, it inhibits autophagy by activating mTORC1 [31]. In addition, p62 can form a complex with LC3 II, which in turn to activate the pro-apoptotic factor BID. BID activation ultimately triggers the release of cytochrome *c*, initiating mitochondria-mediated apoptosis [29]. To clarify the regulation of p62 in TM3 cells after treating with cordycepin, radiation, or their combination, western blotting was used to detect the expression levels of p62 protein at various time points (Fig. 7A). The quantitative result shows that the p62 expressions significantly increased in TM3 cells treated with cordycepin, radiation, or their combination at 24 and 48 h, compared to the untreated control group ($P < 0.05$) (Fig. 7B). In the combination treatment group, p62 expression was notably 3.3-fold higher than in the control group and also higher than in the groups treated with either cordycepin or radiation alone at 48 h.

### *3.8. Cordycepin and radiation induce apoptosis in TM3 cells*

To further confirm whether the cell death induced by cordycepin and radiation in TM3 cells proceeds via apoptosis, Annexin V/PI staining assay was conducted and analyzed using flow cytometry. Fig. 8A shows that both Annexin V+/PI- (lower right quadrant; early apoptotic cells) and Annexin V+/PI+ (upper right quadrant; late apoptotic cells) cell populations were increased by time in TM3 cells treated with cordycepin, radiation, or their combination, indicating that apoptosis was induced after TM3 cells receiving these treatments. Significant increase of apoptotic cell percentage was detected in TM3 cells treated with cordycepin alone and radiation alone at 48 and 72 h, compared to the untreated control group ($P < 0.05$) (Fig. 8B). Moreover, TM3 cells receiving the combination treatment exhibited a notable increase in apoptotic cell percentage as early as 24 h, extending through 48 and 72 h, with approximately half of the cells undergoing apoptosis at 72 h ($P < 0.05$) (Fig. 8B).

## 4. Discussion

Radiotherapy is a localized treatment method commonly utilized in clinical therapeutic strategies for various cancer treatments. However, tumor cells may develop resistance to radiation, thereby reducing their susceptibility to radiotherapy [10]. Our recent research findings have revealed that cordycepin can enhance the radiosensitivity of MA-10 mouse Leydig tumor cells by modulating five different but interrelated mechanisms, including cell cycle arrest, the caspase pathway, ER stress, ROS accumulation, and DNA damage, to induce apoptosis [17,18]. The combination treatment of 4 Gy radiation plus 25 μM cordycepin significantly increased the ratios of MA-10 cells in the sub-G1 and G2/M phases while decreasing the ratios in the S and G1 phases. This modulation was achieved via the regulation of cyclins and cyclin-dependent kinases (CDKs) expression, such as the down-regulation of cyclin E1 and CDK4 expression. Enhanced expression of cleaved caspase-3/-8/-9

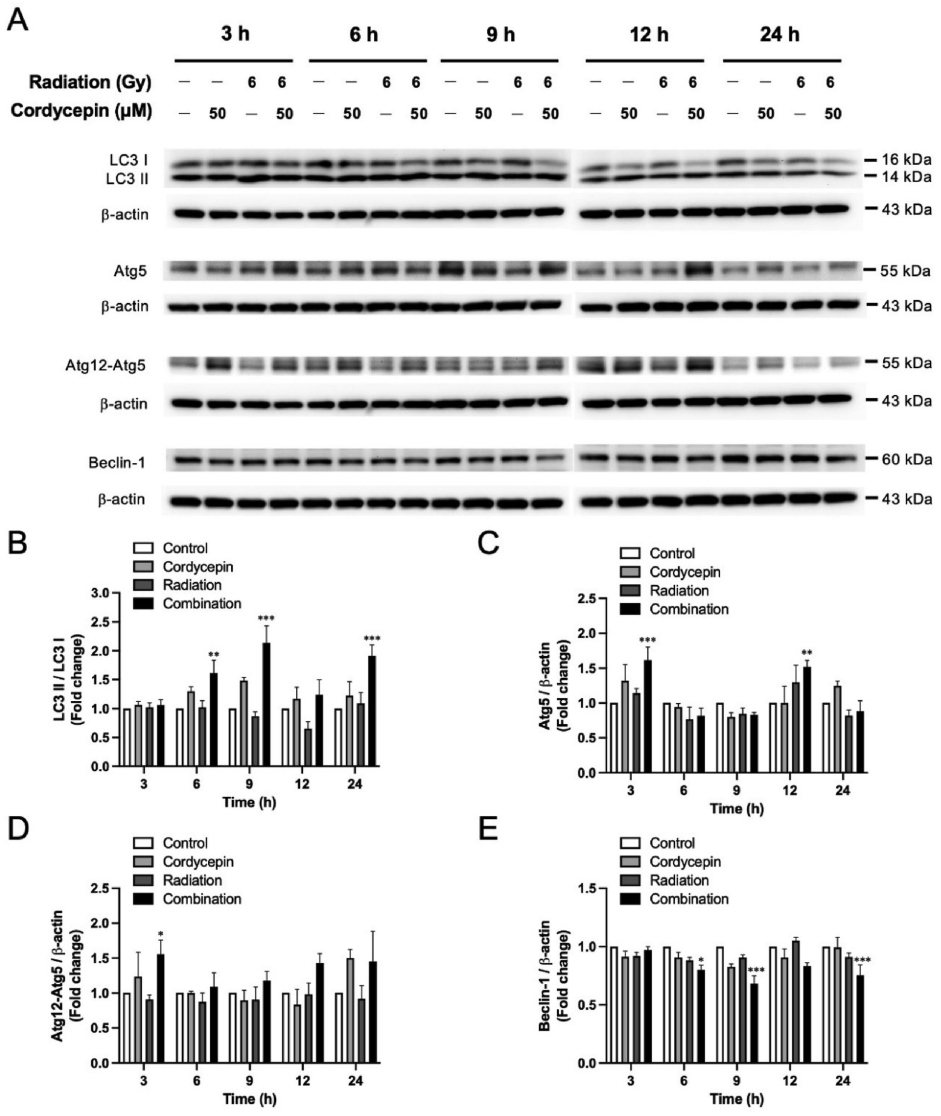


*Fig. 6. Cordycepin and radiation regulate autophagy-related protein expressions in TM3 cells. TM3 cells were treated without or with 50 μM cordycepin, 6 Gy radiation, or 50 μM cordycepin plus 6 Gy radiation for 3, 6, 9, 12, and 24 h, respectively. The protein expression levels of LC3 (LC3 I: 16 kDa; LC3 II: 14 kDa), Atg5 (55 kDa), Atg12-Atg5 (55 kDa), Beclin-1 (60 kDa), and β-actin (43 kDa) were detected by western blotting. The experiment was repeated three times, and (A) a representative result is presented. (B) The integrated optical densities of LC3 II protein expression were normalized with corresponding LC3 I proteins expression in each lane. The integrated optical densities of (C) Atg5, (D) Atg12-Atg5, and (E) Beclin-1 protein expressions were normalized with corresponding β-actin protein expression in each lane. Data are presented as mean ± SEM of three independent experiments. *P < 0.05, **P < 0.01, and ***P < 0.001 indicate significant statistical difference compared to the control group.*

and PARP, cytochrome *c*, glucose-regulated protein (GRP78), phosphorylated-eukaryotic transition initiation factor 2α (p-EIF2α), and CCAAT-enhancer-binding protein homologous protein (CHOP), along with reduced levels of the anti-apoptotic protein Bcl-2, was observed in MA-10 cells following the combination treatment indicating that these cells undergo apoptosis via the induction of caspase pathway and ER stress. Furthermore, the combination treatment also induced intracellular ROS accumulation accompanied by downregulation of heme oxygenase-1 (HO-1) protein expression. Subsequently, it causes single-stranded and double-stranded DNA break through the activation of ataxia telangiectasia mutated (ATM)/checkpoint kinase (Chk)2 and ataxia telangiectasia mutated and Rad3 related (ATR)/Chk1 signaling pathways, respectively, along with a decrease in the expression of phosphorylated H2A histone family member X (γ-H2AX). Eventually, the p53-dependent pathway is activated, prompting the cells towards apoptosis. In the

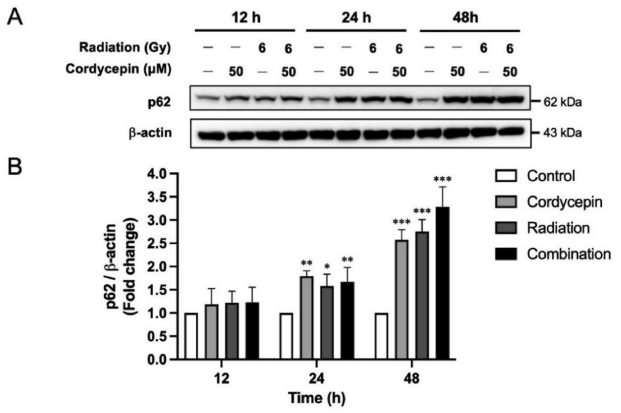


*Fig. 7. Cordycepin and radiation induce p62 protein accumulation in TM3 cells. TM3 cells were treated without or with 50 μM cordycepin, 6 Gy radiation, or 50 μM cordycepin plus 6 Gy radiation for 12, 24, and 48 h, respectively. The protein expression levels of p62 (62 kDa), and β-actin (43 kDa) were detected by western blotting. The experiment was repeated three times, and (A) a representative result is presented. The integrated optical densities of p62 protein expression were normalized with corresponding β-actin protein expression in each lane (B). Data are presented as mean ± SEM of three independent experiments. *P < 0.05, **P < 0.01, and ***P < 0.001 indicate significant statistical difference compared to the control group.*

present study, TM3 Leydig progenitor cells that received the same combination treatment under relative higher dosage condition also showed a significant augmented percentage in sub-G1 and G2/M phases with a decreased percentage of G1 and S phase in the cell cycle progression (Fig. 3). Moreover, due to the p62 accumulation (Fig. 7), these cells may ultimately undergo apoptosis (Fig. 8). However, it needs 1.5-fold higher dosage of radiation and 2-fold higher concentration of cordycepin to induce 50% TM3 Leydig progenitor cell death as compared to the conditions used in MA-10 Leydig tumor cells of previous studies [17,18], reflecting that normal Leydig cells are more resistant to the combination treatment than Leydig tumor cells. As we know, the selective toxicity of cancer treatment strategies to cancer cells versus normal cells is crucial for both efficacy and safety. It gives possibilities in design an effective and safe combination treatment dosages of radiation plus cordycepin based on the sensitivity difference observed between normal Leydig cells and Leydig tumor cells in this study.

Increasing evidence indicates that cordycepin can improve cellular biofunction damage caused by diseases or chemicals through inducing protective autophagy [46–48]. On the other hand, the induction of autophagy also plays a key role in cell protection when cells face chemotherapy drugs [49,50]. Similarly, upon exposure of cells to radiation, induction of autophagy is also often cytoprotective [51,52]. Autophagy-induced resistance to interventional therapeutic strategies may be achieved through a variety of mechanisms, such as enhancing drug or harmful metabolite efflux through overexpression of certain types of transporters, activating metabolic or antioxidant mechanisms, acquiring regulatory control in apoptotic pathways or cell cycle checkpoint or activation of DNA repair mechanisms to reduce DNA damage induced by therapeutic intervention [53]. Accordingly, our data show that the combination treatment induced autophagy in TM3 cells (Fig. 4), accompanied by the upregulation of autophagy-related protein expression levels and the LC3 I/II conversion feature (Fig. 6). Further functional analysis demonstrated that the inhibition of autophagy by pre-incubation with CQ markedly increased the combination treatment-induced cell death (Fig. 5), suggesting that the combination treatment-induced autophagy plays a protective role in TM3 cells. This phenomenon may be the main reason why TM3 cells are more resistant to the combination treatment than MA-10 cells. The protective autophagy induced by the combination treatment in normal Leydig cells provides an optimal entry point for drug development, which could improve the selective toxicity of treatment strategies to ensure safety.

Mechanistically, once autophagy is initiated, Atg5 is covalently linked to Atg12, a ubiquitin-like protein, forming the Atg12–Atg5 conjugate, which is involved in phagophore expansion [54]. The expression level of LC3 II correlates with the number of autophagosomes. Therefore, the ratio of LC3 I to LC3 II conversion can serve as an indicator of autophagic activity [55]. In the results of present study, the expression levels of Atg5 and Atg12-Atg5 complex were increased significantly and were detected as early as 3 h after TM3 cells treating with cordycepin plus radiation (Fig. 6A–D). In addition, the ratio of LC3 I to LC3 II conversion was also detected to be upregulated at 6, 9, and 24 h in TM3 cells treated with the combination treatment (Fig. 6A and B). This evidence confirms that autophagy is initiated as early as 3 h after TM3 cell receiving the combination treatment and persists for at least 24 h, as shown in the data from Fig. 4, approximately 70% of cells undergo autophagy at 24 h in the combination treatment group. Beclin-1 is a key protein in the autophagy process, involved in the formation, expansion, and maturation of phagophore [54]. It recruits and activates other autophagy-related proteins, such as Atg14, to regulate the balance of cellular autophagy (54). The Beclin-1

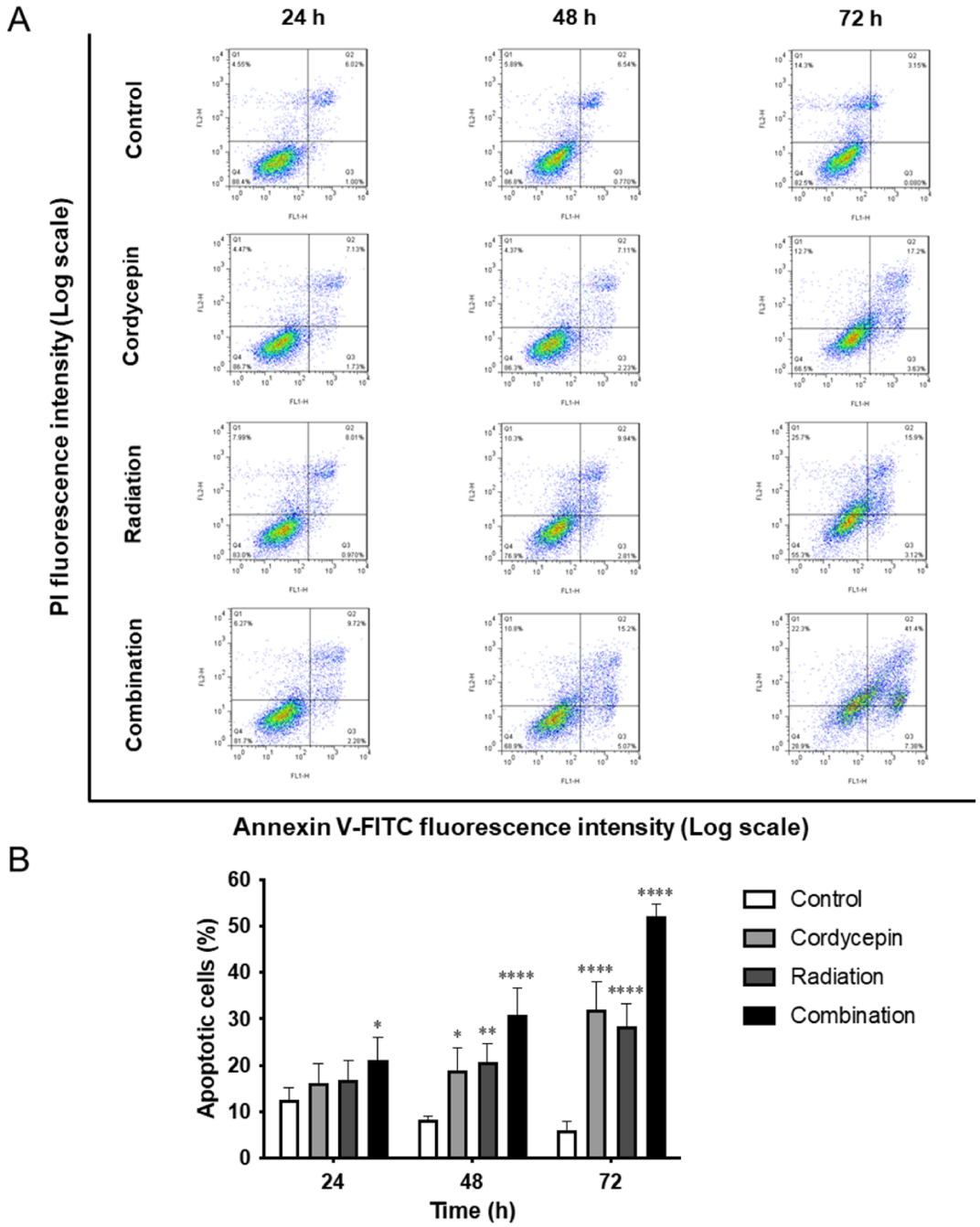


*Fig. 8. Cordycepin and radiation induce apoptosis in TM3 cells. TM3 cells were treated without or with 50 μM cordycepin, 6 Gy radiation, or 50 μM cordycepin plus 6 Gy radiation for 24, 48, and 72 h, respectively. Cells were stained with annexin-V-FITC and propidium iodide (PI). (A) The fractions of viable cells (annexin V-FITC −, PI −; lower left quadrant), necrotic cells (annexin V-FITC −, PI +; upper left quadrant), early apoptotic cells (annexin V-FITC +, PI −; lower right quadrant), and late apoptotic cells (annexin V-FITC +, PI +; upper right quadrant) were determined by flow cytometry. The experiment was repeated three times, and the original density plots of a representative result are presented. The horizontal axis represents the annexin V-FITC fluorescence intensity, and the vertical axis shows the PI fluorescence intensity. (B) Percentages of apoptotic cells are calculated, and data are presented as mean ± SEM of three independent experiments. *P < 0.05, **P < 0.01, and ****P < 0.0001 indicate significant statistical difference compared to the control group.*

expression is downregulated in TM3 cells at 6 h after receiving the combination treatment, indicating a negative regulation of autophagy (Fig. 6A−E). Furthermore, the p62 protein is incorporated into autophagosomes by binding to LC3 II and is efficiently degraded within the autophagosome [54]. Therefore, the total level of p62 is negatively correlated with autophagic flux [56]. We found that p62

accumulation significantly increased over time from 24 h in TM3 cells treated with cordycepin, radiation, or their combination (Fig. 7), which indicates that autophagic degradation and the fusion between autophagosomes and lysosomes were probably inhibited. Excess accumulation of p62 might result in the deactivation of mTORC1 or the induction of oxidative stress, ultimately causing cell damage [31].

Autophagy-induced cell death can be classified into autophagy-dependent cell death (ADCD) that relies on the autophagy mechanism and autophagy-mediated cell death (AMCD) that relies on other mechanisms, for instance, apoptosis [27]. There are three possibilities of the interactions between autophagy and apoptosis including autophagy inhibiting apoptosis, autophagy promoting apoptosis, and both processes being activated independently without influencing each other [27]. Previous studies have revealed that autophagy can promote apoptosis by engulfing apoptosis-related molecules or by directly binding to apoptotic molecules [27,57]. The autophagy product p62 can bind to Fas-associated phosphatase-1 (Fap-1), a negative regulator of Fas, leading to the degradation of Fap-1. Its degradation can promote the phosphorylation of Fas, thereby enhancing the Fas-induced apoptosis [58]. Furthermore, an excess of the p62-LC3 II complex can activate the pro-apoptotic BID protein, thereby initiating mitochondria-mediated apoptosis [29]. Under normal physiological conditions, Atg5 and Atg12 are degraded in a proteasome-dependent manner during the late stages of autophagy [28,59]. If Atg12 is not efficiently degraded, the accumulated Atg12 can bind to and inactivate the anti-apoptotic proteins Bcl-2 and myeloid cell leukemia-1 (Mcl-1) through its BH3-like motif. This inactivation promotes the release of cytochrome *c* from mitochondria and induce apoptosis [60]. Atg5-induced apoptosis is associated with calpain, which cleaves Atg5 into truncated Atg5. The truncated Atg5 can move into the mitochondria to inactivate Bcl-2 and Mcl-1, altering the permeability of the mitochondrial outer membrane and triggering the activation of the caspase cascade [61]. In this study, the combination treatment of cordycepin and radiation induces both autophagy and apoptosis in TM3 cells. However, the crosstalk between these two mechanisms and the molecular mechanisms involved still require further clarification.

When conducting pharmacological and toxicological studies on Leydig cell treatment strategies, the choice of cell lines is relatively limited [1]. TM3 and MA-10 are currently the two most widely utilized cell lines in this field. Both cell lines have physiological properties like native Leydig cells, particularly in hormone response and steroidogenesis [62]. The TM3 cell line better exhibits characteristics similar to those of normal Leydig cell differentiation [38,39]. It is frequently used in studies of Leydig cell function regulation [63], signaling pathways [64], and the differentiation process [41]. Furthermore, it is suitable as a cellular model for drug screening and toxicological research [65]. Therefore, we used MA-10 and TM3 cell lines as Leydig cell tumors and normal Leydig cell models in the previous studies [17,18] and the current study, respectively, to evaluate the impact of the combination treatment of cordycepin and radiation on Leydig cells. One of the current limitations in research is the scarcity of available experimental models. Future research should aim to develop stable primary Leydig cell models for more detailed *ex vivo* analysis. In addition, developing a well-established orthotopic Leydig tumor animal model is also necessary for *in vivo* pharmacological and toxicological assessments of the combination treatment of cordycepin and radiation on Leydig tumor cells and normal Leydig cells.

Current clinical applications of cordycepin are basically in explorative stage, principally on its potential roles upon anti-inflammation [15,16], neuroprotection [66], reproduction [67], and cancer therapy [18,68], in an adjunct status. However, the preclinical investigations of cordycepin illustrate its high potential roles to increase immune responses, decrease inflammations, and suppress tumor growths.

In conclusion, the current study bridges the gap in scientific evidence concerning the effects of the combined cordycepin and radiotherapy on normal Leydig cells during the treatment of Leydig cell tumors. The findings reveal that TM3 Leydig progenitor cells exhibit greater resistance to the combination treatment compared to MA-10 Leydig tumor cells. Following the combination treatment under relatively high-dose, TM3 cells still experience sub-G1 and G2/M phase cell cycle arrest and may undergo apoptosis due to Beclin-1 down-regulation and p62 accumulation. However, protective autophagy is promptly induced early in the treatment process, as evidenced by the upregulation of autophagy-related proteins like LC3 II, Atg5, and the Atg12-Atg5 complex. These results provide valuable insights for designing optimal dosages and improving the combination treatment of cordycepin and radiation for treating Leydig cell tumors.

## Patient consent for publication

Not applicable.

## Availability of data and materials

The datasets used and/or analyzed during the current study are available from the corresponding author on reasonable request.

## Authors' contributions

YYL, YPL, WRH, and CHL designed and conducted the experiments, interpreted results, and wrote the manuscript. LJH, CYY, CHL and BMH participated in the design and coordination of the present study. YYL, YPL, LJH, CHL and BMH were involved in the statistical analysis of results and revised manuscript for substantive and methodological correctness. CYY, CHL and BMH confirm the authenticity of all the raw data. All authors read and approved the final manuscript.

## Ethics approval and consent to participate

Not applicable.

## Funding

The present study was supported by the National Science and Technology Council, Taiwan, ROC. (grant nos. NSTC 110-2320-B-006-025-MY3 and NSTC 113-2320-B-006-041 to BMH; NSTC 111-2811-B-006-018 and SZPT114013 to YPL; NSTC 113-2314-B-194-001 to CYY; and DTCRD114(2)-C-06 to CHL and BMH).

## Competing interests

The authors declare that they have no competing interests.

## Acknowledgements

The authors are grateful for the support from the Core Research Laboratory, College of Medicine, National Cheng Kung University.

## References

[1] Zirkin BR, Papadopoulos V. Leydig cells: formation, function, and regulation. Biol Reprod 2018;99:101−11.
[2] Neaves WB. Leydig cells. Contraception 1975;11:571−606.
[3] Jiang K, Jorgensen JS. Fetal Leydig cells: what we know and what we don't. Mol Reprod Dev 2024;91:e23739.
[4] Heinrich A, DeFalco T. Essential roles of interstitial cells in testicular development and function. Andrology 2020;8:903−14.
[5] Barsoum IB, Yao HH. Fetal Leydig cells: progenitor cell maintenance and differentiation. J Androl 2010;31:11−5.
[6] Maxwell F, Savignac A, Bekdache O, Calvez S, Lebacle C, Arama E, et al. Leydig cell tumors of the testis: an update of the imaging characteristics of a not so rare lesion. Cancers (Basel) 2022;14:3652.
[7] Jou P, Maclennan GT. Leydig cell tumor of the testis. J Urol 2009;181:2299−300.
[8] Bozzini G, Ratti D, Carmignani L. Treatment of leydig cell tumours of the testis: can testis-sparing surgery replace radical orchidectomy? Results of a systematic review. Actas Urol Esp 2017;41:146−54.
[9] Kliesch S. Diagnosis and treatment of Leydig cell tumors. Urologe A 2021;60:880−5.
[10] Baskar R, Lee KA, Yeo R, Yeoh KW. Cancer and radiation therapy: current advances and future directions. Int J Med Sci 2012;9:193−9.
[11] Azzam EI, Jay-Gerin JP, Pain D. Ionizing radiation-induced metabolic oxidative stress and prolonged cell injury. Cancer Lett 2012;327:48−60.
[12] Jia S, Ge S, Fan X, Leong KW, Ruan J. Promoting reactive oxygen species generation: a key strategy in nanosensitizer-mediated radiotherapy. Nanomedicine (Lond) 2021;16:759−78.
[13] Rowley MJ, Leach DR, Warner GA, Heller CG. Effect of graded doses of ionizing radiation on the human testis. Radiat Res 1974;59:665−78.
[14] Tuli HS, Sharma AK, Sandhu SS, Kashyap D. Cordycepin: a bioactive metabolite with therapeutic potential. Life Sci 2013;93:863−9.
[15] Shashidhar MG, Giridhar P, Udaya Sankar K, Manohar B. Bioactive principles from Cordyceps sinensis: a potent food supplement-a review. J Funct Foods 2013;5:1013−30.
[16] Tan L, Song X, Ren Y, Wang M, Guo C, Guo D, et al. Anti-inflammatory effects of cordycepin: a review. Phytother Res 2020;35:1284−97.
[17] Lee YP, Huang WR, Wu WS, Wu YH, Ho SY, Wang YJ, et al. Cordycepin enhances radiosensitivity to induce apoptosis through cell cycle arrest, caspase pathway and ER stress in MA-10 mouse Leydig tumor cells. Am J Cancer Res 2022;12:3601−24.
[18] Lee YP, Lin CR, Chen SS, Chen RJ, Wu YH, Chen YH, et al. Combination treatment of cordycepin and radiation induces MA-10 mouse Leydig tumor cell death via ROS accumulation and DNA damage. Am J Cancer Res 2023;13:1329−46.
[19] Sun Y, Liu Y, Ma X, Hu H. The influence of cell cycle regulation on chemotherapy. Int J Mol Sci 2021;22:6923.
[20] Williams GH, Stoeber K. The cell cycle and cancer. J Pathol 2012;226:352−64.
[21] Otto T, Sicinski P. Cell cycle proteins as promising targets in cancer therapy. Nat Rev Cancer 2017;17:93−115.
[22] Smith HL, Southgate H, Tweddle DA, Curtin NJ. DNA damage checkpoint kinases in cancer. Expert Rev Mol Med 2020;22:e2.
[23] Evan GI, Brown L, Whyte M, Harrington E. Apoptosis and the cell cycle. Curr Opin Cell Biol 1995;7:825−34.
[24] Xu B, Kim ST, Lim DS, Kastan MB. Two molecularly distinct G(2)/M checkpoints are induced by ionizing irradiation. Mol Cell Biol 2002;22:1049−59.
[25] Glick D, Barth S, Macleod KF. Autophagy: cellular and molecular mechanisms. J Pathol 2010;221:3−12.
[26] Das G, Shravage BV, Baehrecke EH. Regulation and function of autophagy during cell survival and cell death. Cold Spring Harb Perspect Biol 2012;4:a008813.
[27] Liu S, Yao S, Yang H, Liu S, Wang Y. Autophagy: regulator of cell death. Cell Death Dis 2023;14:648.
[28] Saha S, Panigrahi DP, Patil S, Bhutia SK. Autophagy in health and disease: a comprehensive review. Biomed Pharmacother 2018;104:485−95.
[29] Yang J, Moon HG, Chettimada S, Jin Y. Cross-talk between apoptosis and autophagy in lung epithelial cell death. J Biochem Pharmacol Res 2014;2:99−109.
[30] Moscat J, Diaz-Meco MT. p62 at the crossroads of autophagy, apoptosis, and cancer. Cell 2009;137:1001−4.
[31] Komatsu M, Kageyama S, Ichimura Y. p62/SQSTM1/A170: physiology and pathology. Pharmacol Res 2012;66:457−62.
[32] Letai A, Bassik MC, Walensky LD, Sorcinelli MD, Weiler S, Korsmeyer SJ. Distinct BH3 domains either sensitize or

activate mitochondrial apoptosis, serving as prototype cancer therapeutics. Cancer Cell 2002;2:18392.
[33] Elmore S. Apoptosis: a review of programmed cell death. Toxicol Pathol 2007;35:495–516.
[34] Xu X, Lai Y. Hua ZC: apoptosis and apoptotic body: disease message and therapeutic target potentials. Biosci Rep 2019; 39:BSR20180992.
[35] Newton K, Strasser A, Kayagaki N, Dixit VM. Cell death. Cell 2024;187:235–56.
[36] Saraste A, Pulkki K. Morphologic and biochemical hallmarks of apoptosis. Cardiovasc Res 2000;45:528–37.
[37] Matassov D, Kagan T, Leblanc J, Sikorska M, Zakeri Z. Measurement of apoptosis by DNA fragmentation. Methods Mol Biol 2004;282:1–17.
[38] Mather JP, Zhuang LZ, Perez-Infante V, Phillips DM. Culture of testicular cells in hormone-supplemented serum-free medium. Ann N Y Acad Sci 1982;383:44–68.
[39] Mather JP. Establishment and characterization of two distinct mouse testicular epithelial cell lines. Biol Reprod 1980;23:243–52.
[40] Ham J, Lim W, Whang KY, Song G. Butylated hydroxytoluene induces dysregulation of calcium homeostasis and endoplasmic reticulum stress resulting in mouse Leydig cell death. Environ Pollut 2020;256:113421.
[41] Chang MM, Weng HY, Lai MS, Wang LW, Yang SH, Wu CC, et al. FGF9 promotes cell proliferation and tumorigenesis in TM3 mouse Leydig progenitor cells. Am J Cancer Res 2022;12:5613–30.
[42] Ge JC, Qian Q, Gao YH, Zhang YF, Li YX, Wang X, et al. Toxic effects of Tripterygium glycoside tablets on the reproductive system of male rats by metabolomics, cytotoxicity, and molecular docking. Phytomedicine 2023;114: 154813.
[43] Chou TC, Talalay P. Quantitative analysis of dose-effect relationships: the combined effects of multiple drugs or enzyme inhibitors. Adv Enzyme Regul 1984;22:27–55.
[44] Chen YY, Chen CH, Lin WC, Tung CW, Chen YC, Yang SH, et al. The role of autophagy in anti-cancer and health promoting effects of cordycepin. Molecules 2021;26:4954.
[45] Panganiban RA, Snow AL, Day RM. Mechanisms of radiation toxicity in transformed and non-transformed cells. Int J Mol Sci 2013;14:15931–58.
[46] Cao T, Xu R, Xu Y, Liu Y, Qi D, Wan Q. The protective effect of cordycepin on diabetic nephropathy through autophagy induction in vivo and in vitro. Int Urol Nephrol 2019;51: 1883–92.
[47] Li T, Wen L, Cheng B. Cordycepin alleviates hepatic lipid accumulation by inducing protective autophagy via PKA/mTOR pathway. Biochem Biophys Res Commun 2019;516: 632–8.
[48] Li J, Zhong L, Zhu H, Wang F. The protective effect of cordycepin on D-galactosamine/lipopolysaccharide-induced acute liver injury. Mediators Inflamm 2017;2017:3946706.
[49] Li YJ, Lei YH, Yao N, Wang CR, Hu N, Ye WC, et al. Autophagy and multidrug resistance in cancer. Chin J Cancer 2017;36:52.
[50] Antunes F, Erustes AG, Costa AJ, Nascimento AC, Bincoletto C, Ureshino RP, et al. Autophagy and intermittent fasting: the connection for cancer therapy? Clinics (Sao Paulo) 2018;73:e814s.
[51] Zheng Z, Wang L, Cheng S, Wang Y, Zhao W. Autophagy and lymphoma. Adv Exp Med Biol 2020;1207:615–23.
[52] Xin Y, Jiang F, Yang C, Yan Q, Guo W, Huang Q, et al. Role of autophagy in regulating the radiosensitivity of tumor cells. J Cancer Res Clin Oncol 2017;143:2147–57.
[53] Kocaturk NM, Akkoc Y, Kig C, Bayraktar O, Gozuacik D, Kutlu O. Autophagy as a molecular target for cancer treatment. Eur J Pharm Sci 2019;134:116–37.
[54] Boya P, Reggiori F, Codogno P. Emerging regulation and functions of autophagy. Nat Cell Biol 2013;15:713–20.
[55] Mizushima N, Yoshimori T, Levine B. Methods in mammalian autophagy research. Cell 2010;140:313–26.
[56] Huang SP, Chien JY, Tsai RK. Ethambutol induces impaired autophagic flux and apoptosis in the rat retina. Dis Model Mech 2015;8:977–87.
[57] Lin L, Baehrecke EH. Autophagy, cell death, and cancer. Mol Cell Oncol 2015;2:e985913.
[58] Gump JM, Staskiewicz L, Morgan MJ, Bamberg A, Riches DW, Thorburn A. Autophagy variation within a cell population determines cell fate through selective degradation of Fap-1. Nat Cell Biol 2014;16:47–54.
[59] Haller M, Hock AK, Giampazolias E, Oberst A, Green DR, Debnath J, et al. Ubiquitination and proteasomal degradation of ATG12 regulates its proapoptotic activity. Autophagy 2014;10:2269–78.
[60] Rubinstein AD, Eisenstein M, Ber Y, Bialik S, Kimchi A. The autophagy protein Atg12 associates with antiapoptotic Bcl-2 family members to promote mitochondrial apoptosis. Mol Cell 2011;44:698–709.
[61] Yousefi S, Perozzo R, Schmid I, Ziemiecki A, Schaffner T, Scapozza L, et al. Calpain-mediated cleavage of Atg5 switches autophagy to apoptosis. Nat Cell Biol 2006;8: 1124–32.
[62] Engeli RT, Fürstenberger C, Kratschmar DV, Odermatt A. Currently available murine Leydig cell lines can be applied to study early steps of steroidogenesis but not testosterone synthesis. Heliyon 2018;4:e00527.
[63] Taylor CC, Limback D, Terranova PF. Src tyrosine kinase activity in rat thecal-interstitial cells and mouse TM3 Leydig cells is positively associated with cAMP-specific phosphodiesterase activity. Mol Cell Endocrinol 1997;126:91–100.
[64] Doepner RF, Geigerseder C, Frungieri MB, Gonzalez-Calvar SI, Calandra RS, Raemsch R, et al. Insights into GABA receptor signalling in TM3 Leydig cells. Neuroendocrinology 2005;81:381–90.
[65] Han JW, Park HJ. Perfluorooctanoic acid induces cell death in TM3 cells via the ER stress-mitochondrial apoptosis pathway. Reprod Toxicol 2023;118:108383.
[66] Tung CW, Chan SC, Cheng PH, Chen YC, Wu PM, Lin WC, et al. Exploring cordycepin as a neuroprotective agent in Huntington's disease: in vitro and in vivo insights. Pharmacol Res Perspect 2025;13(2):e70091.
[67] Chen YC, Chen YH, Pan BS, Chang MM, Huang BM. Functional study of Cordyceps sinensis and cordycepin in male reproduction: a review. J Food Drug Anal 2017;25: 197–205.
[68] Chen LC, Chen CY, Lee YP, Huang BM. Cordycepin inhibits ERK pathway to suppress FGF9-induced tumorigenesis with MA-10 mouse Leydig tumor cells. J Food Drug Anal 2023;31:485–501.